Journal of Positive Psychology & Wellbeing
2023, Vol. 7, No. 1, 293-310
http://journalppw.com
ISSN 2587-0130

Correlation between Solar Intensity and Relative Humidity and its Influence on the Performance of Solar Stills

Jhon Jairo Feria-Díaz[1,2], María Cristina López-Méndez[1,*], Lucero Ortiz-Monterde[1]

[1]División de Estudios Posgrado e Investigación, Tecnológico Nacional de México/Instituto Tecnológico Superior de Misantla, Misantla 93821, México; jhon.feria@unisucre.edu.co; monterde9889@gmail.com
[2]Facultad de Ingeniería, Universidad de Sucre, Sincelejo 700001, Colombia
**Correspondence: mclopezm@itsm.edu.mx*

ABSTRACT

Solar stills are thermal devices that can be used in far distant areas or rural communities with freshwater deficits due to their ease of construction and relative cheap costs. Nonetheless, climatic factors can significantly affect performance of these devices and the technical feasibility for their usage. This research assesses solar intensity behavior, relative humidity, cloud cover and the existing correlations between these climatic factors in addition to how they influence a solar still production and performance. Tests were carried out in the city of Misantla, Veracruz State, Mexico; therefore, results cannot be extrapolated to a different latitude. It was found that there is a negative linear correlation between solar intensity and relative humidity of the monitoring site, depending on cloudiness. This negative correlation varies from moderate to high when cloud cover is between 46 and 55%. However, for less than 10% cloud cover, negative linear correlation was very high, with a correlation coefficient higher than -0.90. It was verified that performance of solar stills depends fundamentally on the average solar radiation, cloud cover and duration of the shadow at the test site.

Keywords: solar intensity; relative humidity; cloud cover; solar still; local climatic conditions.

Introduction

The world is facing severe freshwater shortages and only a third of the world's population has access to safe potable water [1]. Annual availability of freshwater has been decreasing day by day in most countries [2]. According to the United Nations (UN), most people live in areas with severe water scarcity; and lack of clean and safe water is one of the main reasons for the spread of transmissible diseases around the world [3]. People living in far distant and rural areas, mainly in developing countries, face serious problems due to lack of education, infrastructure, and limited resources, in addition to the unavailability of the freshwater supply chain [4]. Consequently, serious efforts are being made all over the world to avoid this imminent crisis, starting from the conservation of existing freshwater and obtaining large quantities of freshwater through different technologies of seawater desalination.

Two forms of desalination are: thermal and membrane processes. The thermal process involves physical transformation of water molecules from liquid to vapor (evaporation) and back to liquid through heat condensation, while the membrane process involves separation of salt and other pollutants from seawater through a membrane under pressure, without change in the water state [5,6].

In thermal desalination technologies, saline or brackish water is evaporated using heat energy, and the resulting steam is collected and condensed as the final product [7]. The solar

thermal water desalination method is broadly divided into two main categories: a) direct system and b) indirect system. The key distinction between these desalination methods is that, in a direct system, solar intensity is absorbed and converted to heat to evaporate the salty water within the device. While the indirect system uses dual separate systems: a solar collection array, comprising fluid-based thermal and/or photovoltaic (PV) collectors, and a discrete conventional distillation plant to eliminate loss during the latent heat of condensation [8].

Locations where there is an ample supply of both solar intensity and brackish water allow production of reasonable quantities of potable water at economical cost through solar stills, easily constructed and relatively cheap. This concept is also useful in the context of providing water to rural or remote communities [9]. For a far distant area with scarce freshwater, but abundant amount of solar radiation, the use of solar energy is the preferred alternative energy source. Therefore, solar energy is the most suitable form of energy that can be harnessed to provide cheap potable water using decentralized methods [10].

Conventional solar stills consist mainly of a water tank, generally insulated to reduce heat losses, an absorber plate painted black to maximize absorption of solar radiation, a glass cover placed at an angle facing the sun, a tank supply connected to the inlet of the distiller to supply seawater, a collection tray, and a collection tank connected to the distiller outlet. The rays of sunlight enter through the glass cover, heat penetrates, and the evaporation process occurs [11].

Typically, the maximum efficiency of a conventional solar still is around 50% when fully isolated. Less insulation produces a reduction of approximately 14.5% efficiency [7]. The performance of a solar still depends on the climatic conditions of the place under study, design, and operating parameters [9]. The main drawback of solar desalination using solar stills is low productivity. Commonly, a solar still can produce 2.5 to 5 L/m^2-day of freshwater, and it is considered that the main environmental parameter affecting this productivity rate is incident solar intensity [12]. However, recent studies carried out in Mexico report rates of up to 1.57 L/m^2-day, a production that is below average standards, mainly due to climatic conditions and latitude of the place where the tests were carried out [13]. It is noteworthy that climatic factors are considered meteorological factors not controlled by humans [14,15]. Among the climatic factors affecting freshwater production in solar stills, the following ones are considered:

Solar Radiation

According to technical literature, there is a consensus that solar intensity is the most effective factor in a solar still performance [9,16-21]. The higher the solar radiation, the higher the solar still productivity [20]. Solar intensity heats the water in the basin and increases the convective heat transfer coefficient, causing the water in the basin to rapidly evaporate [21]. When the strength of solar intensity is lowered, the solar still efficiency also decreases at the same time, and this effect is generally observed during the Summer [18]. Solar stills work based on the heating, evaporation, and water condensation to produce freshwater. This indicates that the decrease in the solar intensity would reduce the system productivity [10]. In this sense, Ghoneyem et al. [22] established empirical equations to express the productivity dependence of the solar still on ambient temperature and solar radiation. Therefore, the evaporation rate of the solar still depends on the water mass temperature in the basin, the glass cover temperature, and the difference between the two [23]. Based on the technical literature, it can be concluded that a combination of high solar radiation intensities in regions with high temperatures can provide better productivity in terms of daily distillate production [14]. Consequently, the material of

the condensation cover must be properly selected, since it has an important role in the absorption process of solar radiation, which affects the system performance [24].

Ambient Temperature

Ambient temperature depends on the solar radiation amount that enters the Earth's atmosphere. As the solar intensity increases, the temperature of various parts of the still rises as well [25], including the basin containing the salty water. Due to the temperature difference between the basin and still cover, freshwater production increases in the solar still [26]. Maximum solar radiation occurs at 1:00 p.m. and maximum ambient temperature at 3:00 p.m. This time difference is due to the water thermal capacity, moisture content and density of the surrounding air [27]. Based on a theoretical model proposed by Malik et al. [28] the effect of ambient temperature on the productivity of solar stills has been researched, showing that the higher the ambient temperature, the higher the still's productivity up to 8.2% when ambient temperature increases 10ºC [29].

Wind speed

Effect of wind speed is negligible compared to productivity. Productivity rises with decreasing cover temperature. The temperature difference between glass and water widens as the cover temperature decreases, which consequently improves natural circulation of air mass inside the solar still [9]. Studies carried out by Reddy & Reddy, showed that for the ambient temperature and water inside the still, the coefficient of heat transfer by radiation between water and glass (h_{ewg}) decreased with the rise of wind speed. Similarly, it showed that wind speed is negligible compared to the evaporative heat transfer coefficient between water and glass (h_{rwg}) and, finally, the radiation heat transfer coefficient between glass and ambience (h_{rga}) decreases with the increase in wind speed [30]. On the other hand, El-Sebaii researched the effect of wind speed on the production of active and multi-effect passive solar stills and concluded that the production increases with increasing wind speed [23]. Nevertheless, it was also shown that when wind speed increases from 1 to 9 m/s, the total system performance drops by 13% [18]. Castillo-Téllez et al., based on experiments carried out in a wind tunnel, reported that with speeds of up to 5.5 m/s, production of freshwater in a still is optimal, and beyond that wind speed, production begins to decrease [31]. In this sense, Sharshir et al. also determined that the reduction of ambient air temperature has a positive effect on productivity, while with high wind speeds, there is a negative effect [7]. Even so, research is lacking on the optimal values of wind speed that can increase the total production of freshwater in a still [14].

Location latitude and longitude

Geographical location plays a very important role in the freshwater production of a solar still [32]. Depending on the latitude where the solar still is located, there is an optimal angle of inclination for the glass cover, thus, productivity is maximum when the inclination angle becomes equivalent to the place latitude [33]. However, the optimal angle also varies depending on the seasons. In Summer, as the inclination angle of the solar still cover decreases, the production of freshwater increases, while during winter, productivity rises as the inclination angle increases [18].

Cloud and dust cover

Few studies have been carried out to establish the influence of cloud cover on the average production of freshwater in a solar still. Zamfir et al. conducted in Bucharest, Romania (latitude 44.4 ºN), experiments to find the effect of clouds on a solar still performance. Results showed that freshwater production is lower on cloudy days compared to production on clear days without cloud cover, since cloud cover directly affects the solar radiation amount absorbed in the still [34]. Conversely, most of the research conducted in dusty environments reveals that productivity is

lowered by these natural phenomena, and subtle precautions can improve productivity [14]. When dust accumulates on the glass cover, transmittance decreases, resulting in loss of incident solar radiation. The amount of incident light is diminished by dust, and its damaging effects depend on a variety of factors. Sandstorms throw a fine layer of dust over the collector or reflector areas, which remain until they are blown or blown away by the wind [2]. El-Nashar et al. reported an annual reduction of 70% in the transmission of solar radiation when the still glass cover is not clean or is not maintained and cleaned [35]. Presence of dust and dirt on the glass cover surface changes the glass optical properties, which affects the absorption and transmission capacity of the cover, which in turn alters the solar still productivity [9].

Relative humidity

Several authors have shown that rises in the site relative humidity where the solar still is located lead to increases in the system performance [36,37]. Kofi et al., based on their studies, stated that increases in relative humidity when the monitoring site has an average humidity of 65% during the rainy seasons, and 40 to 55% during the dry seasons, contributed to the rise in production of solar stills [38].

Therefore, climatic conditions and the place latitude and longitude where solar stills are located, are determining factors in their efficiency, production, and performance. Thus, the primary objective of this research is to evaluate the correlation between solar intensity and relative humidity, depending on cloud cover, in addition to its influence on the freshwater performance and production from a conventional solar still.

2. Materials and Methods

2.1. Study Area Description

This research was carried out at the campus of the Instituto Tecnológico Superior de Misantla ITSM [Higher Technological Institute of Misantla], located in the municipality of Misantla, Mexico. The municipality is in a mountainous area in the center of Veracruz State, at coordinates 19º 56' north latitude and 96º 51' west longitude and at 300 m.a.s.l [39]. In Misantla, the wet season is hot, oppressive, and overcast, and the dry season is hot, humid, and partly cloudy. Temperature generally ranges from 15°C to 32°C during the year and rarely drops below 11°C or rises above 36°C. Figure 1 shows the behavior of the main climatic parameters of the study area.

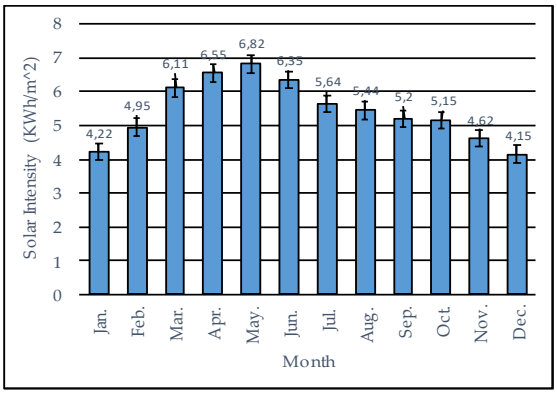

(a)

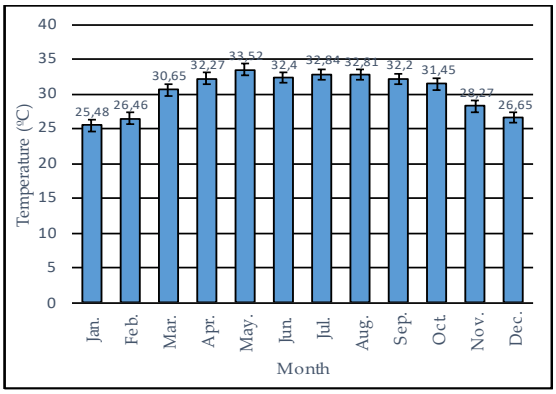

(b)

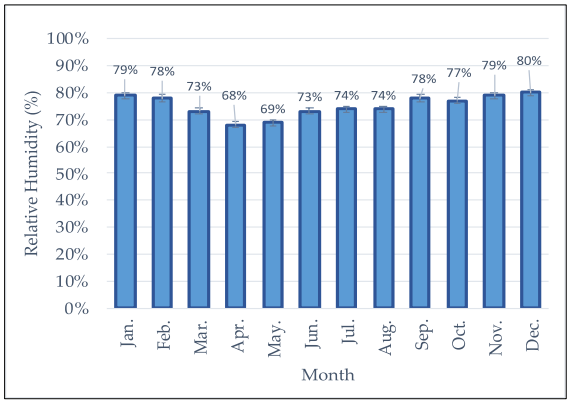

(c)

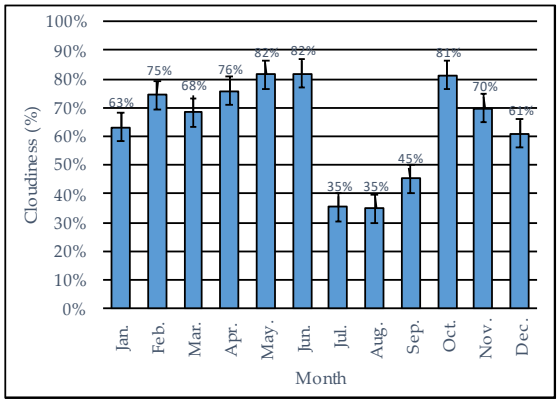

(d)

Figure 1. Average annual climatic behavior in Misantla, Mexico: (a) Solar intensity, (b) Ambient temperature, (c) Relative humidity, and (d) Cloudiness.

Solar radiation or solar intensity defines the solar energy amount that a place on the planet can receive. According to Figure 1a, the brightest period of the year in Misantla lasts 2.7 months, starting in March and ending in June, with an average daily incident shortwave energy above 5.43 kWh. May is the brightest month, averaging 6.9 kWh. In contrast, the darkest period of the year lasts 2.5 months, starting in November and ending in January, with an average value of 4.8 kWh. The darkest month of the year in Misantla is December, with an average value of 4.3 kWh. The ambient temperature in Misantla is a function of the solar intensity it receives and the dry or rainy period in which this parameter is determined. From June to October, the highest temperatures occur, having August, the highest multi-year average records, and February, the lowest temperature records (see Figure 1b).

Perceived humidity varies extremely in Misantla. The month with the highest relative humidity is December (80%). The month with the lowest relative humidity is April (68%). The wettest period of the year lasts 6 months, from September to February (see Figure 1c). Finally, in Misantla, the average percentage of the sky covered with clouds varies considerably throughout the year. The clearer part of the year begins around December and lasts for 7 months, ending around August. The month with the highest number of rainy days is September (22.5 days). The month with the lowest number of rainy days is April (8.1 days) (see Figure 1d).

2.2. Meausurement of Cloud cover

Cloud cover or cloudiness is defined by the World Meteorological Organization (WMO) Code 2700 as the fraction of the total sky covered by clouds, measured in octaves of sky cover [40]. Considering that cloudiness is a factor that directly affects the greater or lesser solar radiation on the earth's surface, its determination is important, since it directly lowers the performance of any solar distillation system [9,41]. The cloud cover correction algorithms of Laevastu [42], Kasten & Czeplak [43], Dobson & Smith [44] and Davis [45] estimate cloud cover as a percentage between the overcast sky and the clear or cloudless sky. This research proposes to measure cloud cover in an indirect and approximate way, quantifying time percentage (minutes) in which the shadow of the clouds is reflected on the place where measurements of solar intensity are taken, such as:

$$\text{Cloud cover} = \frac{\text{Shadow minutes of the monitored day}}{\text{Total minutes of the monitored day}} * 100\% \quad (1)$$

This estimation approach is because cloud cover is still obtained predominantly through human observations [46].

2.3. Field tests and Statistical Data Management

Data used to verify the correlation between solar intensity and relative humidity were taken between August 25 and September 15, 2022. This is a perfect period since there were cloudy and sunny days, depending on the punctual cloudiness of the site where the solar still was located. Field data (solar intensity and relative humidity) were taken from an Ambient Weather smart weather station, model WS-2902C, between 8:00 a.m. and 6:30 p.m., with readings every 5 minutes, throughout the observation period. With the obtained data, a statistical analysis of variance was performed through ANOVA and Fisher's multiple range tests, using the Statgraphics Centurion XVI (Trial Version) software. For all cases, significance level was set at 0.05. A conventional solar still was used to measure performance for a few days of the monitoring period. In Figure 2, the still used to estimate the performance and production of fresh water is shown.

The solar still is 50 cm long and 30 cm high and wide, with walls made of 5 mm thick glass. The metal container for seawater has an area of 0.09 m^2.

Figure 2. Solar still used for the tests

2.4. Statistical Indicators

A linear regression model was used to assess the correlation between solar intensity and relative humidity. The statistical adjustment of the model was measured through Pearson's correlation coefficient matrices (R) and with the determination coefficient (R2). Equations 2 and 3 correspond to these statistical indicators [47,48]:

$$R = \frac{\sum_{i=1}^{n}(y_i - \bar{y_i})(q_i - \bar{q_i})}{\sqrt{\sum_{i=1}^{n}(y_i - \bar{y_i})^2 \ \Sigma(q_i - \bar{q_i})^2}} \quad (2)$$

$$R^2 = \left(\frac{\sum_{i=1}^{n}(y_i - \bar{y_i})(q_i - \bar{q_i})}{\sqrt{\sum_{i=1}^{n}(y_i - \bar{y_i})^2 \ \Sigma(q_i - \bar{q_i})^2}} \right)^2 \quad (3)$$

Where y_i and q_i correspond to the values of each parameter to be assessed, during "i" period; $\bar{y_i}$ and $\bar{q_i}$ are the averages of these parameters and "n" corresponds to the number of data of "i". When R is greater than 0.8, the assessed values are highly correlated. Similarly, an R2 close to 1 indicates that the model values fit very highly [48,49]. An R2 of

0.65 to 0.75 implies outstanding performance, while an R2 less than 0.50 indicates poor performance [50,51].

3. Results

3.1. Behavior of Solar Intensity and Relative Humidity

Solar intensity during the monitored days was plotted using box and whisker plots, and they were analyzed with ANOVAS to verify if there were statistically significant differences between the means of the data. In case of statistically significant differences between some days, according to the results shown by Fisher's multi-parameter test, the homogeneous groups were pooled together.

Figure 3 shows the ranges and means of solar intensity for each day of the observation period. The central line that joins the different boxes corresponds to the average value of radiation reached on each monitored day. Therefore, the average solar intensity was between 250 and 440 W/m^2, with isolated maximum peaks above 1000 W/m^2 on September 14. After previously checking the conditionals of normality, independence, and data homogeneity.

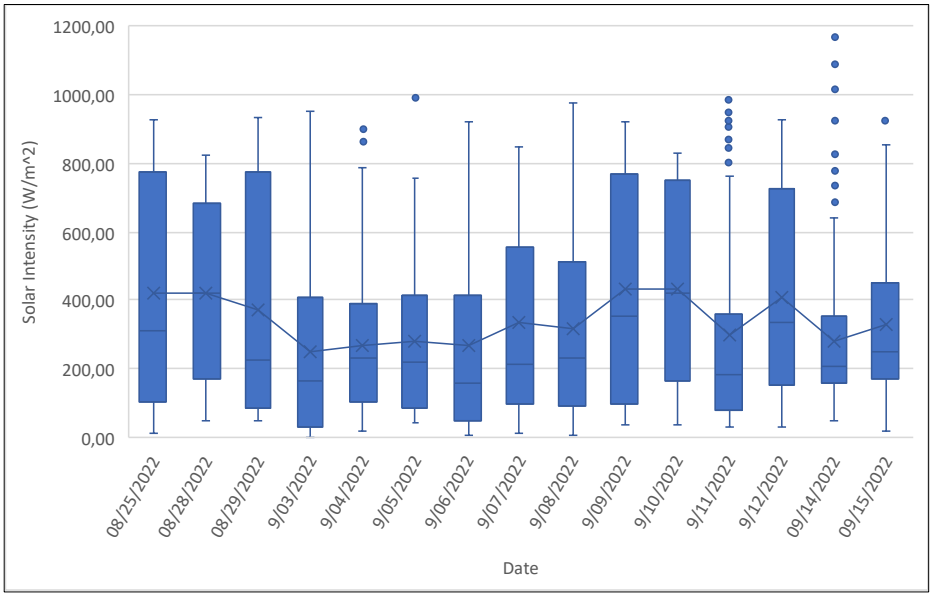

Figure 3. Solar intensity in the study area during the observation days.

Table 1 shows the results found for the ANOVA between the means of solar intensity.

Table 1. ANOVA between means of the solar intensity during the observation days.

Source	Sum of Squares	DF	Mean Squares	F-Value	P-Value
Between	8229023.737	14	587787.4098	8.0236	7.16931E-17
Within Groups	137503816.50	1877	73257.22774		
Total (Corr.)	145732840.20	1891			

Given that the ANOVA P-value is less than 0.05, it is possible to affirm that there is a statistically significant difference between the means of the solar intensity, at least between one day and the other, or several days between them, with a 95 % confidence level. To determine which means are significantly different from others, and define which ones belong to the same homogeneous group, the Fisher Multiple Range Test was applied [52], results of which, are shown in Table 2.

Table 2. Results of the Fisher Multiple Range Test to determine homogeneous groups between means of solar intensity during the observation days.

Date	Cases	Mean	Homogeneous Groups
29/08/22	127	370.851	X
3/09/22	127	247.806	X
14/09/22	127	282.320	X
4/09/22	127	269.326	XX
5/09/22	127	281.557	XX
6/09/22	122	267.265	XX
11/09/22	127	297.946	XX
7/09/22	123	334.369	XXX
8/09/22	127	316.411	XXX
12/09/22	127	411.239	XXX
15/09/22	125	332.564	XXX
25/08/22	125	418.716	XXXX
28/08/22	127	423.337	XXXX
9/09/22	127	433.773	XXXX
10/09/22	127	436.156	XXXX

According to the results shown in Table 2, it is possible to group means into 4 groups of values that do not have statistically significant differences among themselves, with a 95% confidence level. The first group is made up of August 29, September 3 and 14, 2022. The second group is made up of September 4, 5, 6 and 11. The third group is made up of the days 7, 8, 12 and 15 of September. Finally, the fourth group includes the days of August 25 and 28, and September 9 and 10, 2022.

Figures 4 and 5 show the behavior of solar intensity and relative humidity from group 1; and the results of the linear regression model applied to determine if there is a correlation between the studied parameters, respectively.

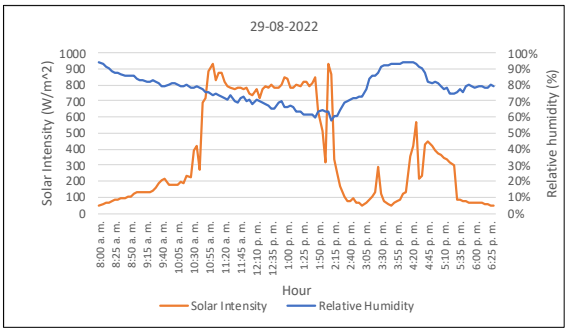

(**a**)

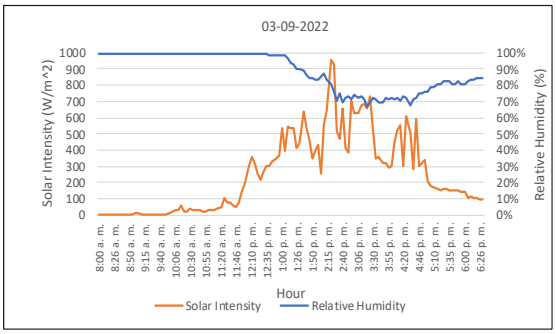

(**b**)

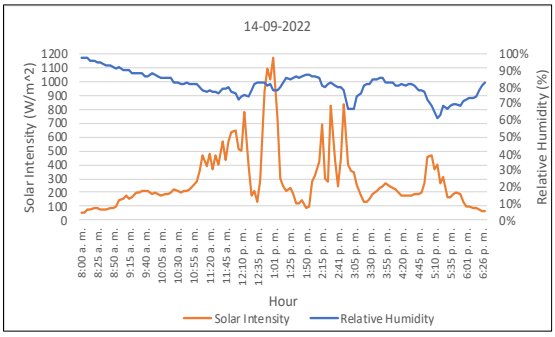

(**c**)

Figure 4. Behavior of solar intensity and relative humidity, group 1: (a) 08/29/2022, (b) 09/03/2022, and (c) 09/14/2022.

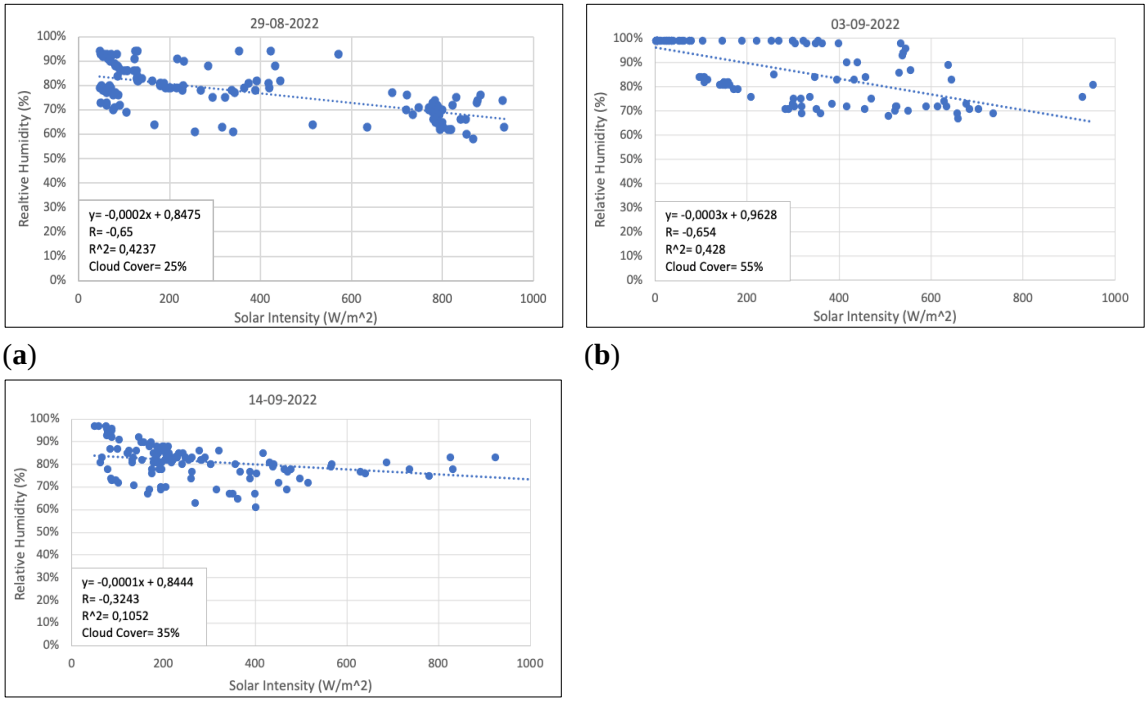

Figure 5. Linear regression model and cloud cover, group 1: (a) 08/29/2022, (b) 09/03/2022, and (c) 09/14/2022.

In this group, there were rainy events throughout the day, and high and prolonged cloud cover. On August 29, a sunny morning was observed, with low cloud cover, which allowed high solar intensity between 10:45 am and 1:45 pm, with radiation between 690 and 931 W/m^2. Nonetheless, from 2:15 pm to 4:20 pm, there were rain events, followed by prolonged cloud cover at the end of the observation day (see Figure 4a). On September 3, rains occurred in the morning, followed by high cloudiness throughout the day, although isolated radiation peaks of 952 W/m^2 were achieved in the afternoon at 2:20 pm (See Figure 4b). On the last day of this group, two rain events were observed: the first between 1:10 and 2:25 pm, and the second between 3:00 and 5:00 pm, accompanied by high and prolonged coverage of cloudiness throughout the day. However, on this day and in isolation, the highest peaks of solar intensity (up to 1166 W/m^2) were recorded between 12:00 and 1:00 pm (see Figure 4c).

According to the applied linear regression model and the results of the Pearson correlation matrix, shown in Figure 5, all the R of this

group are less than -0.8, which implies that there is not a high linear correlation between solar intensity and relative humidity during those observation days. On August 29 and September 3, an R coefficient of -0.65 was found, indicating a moderate negative linear correlation between these two parameters; while on September 14, it showed an R of -0.32, i.e., a low negative linear correlation [53]. Similarly, R^2 showed a poor performance of the applied linear regression model. This behavior between solar intensity and relative humidity may be associated with rain events and the prolonged cloud cover that occurred during those observation days. Particularly, the low negative correlation on September 14 could be due to the two rain events that strongly increased and prolonged cloud cover, and consequently, the low solar intensity at the study site.

Figures 6 and 7 show the behavior of solar intensity and relative humidity in addition to the linear regression model for days of group 2, respectively.

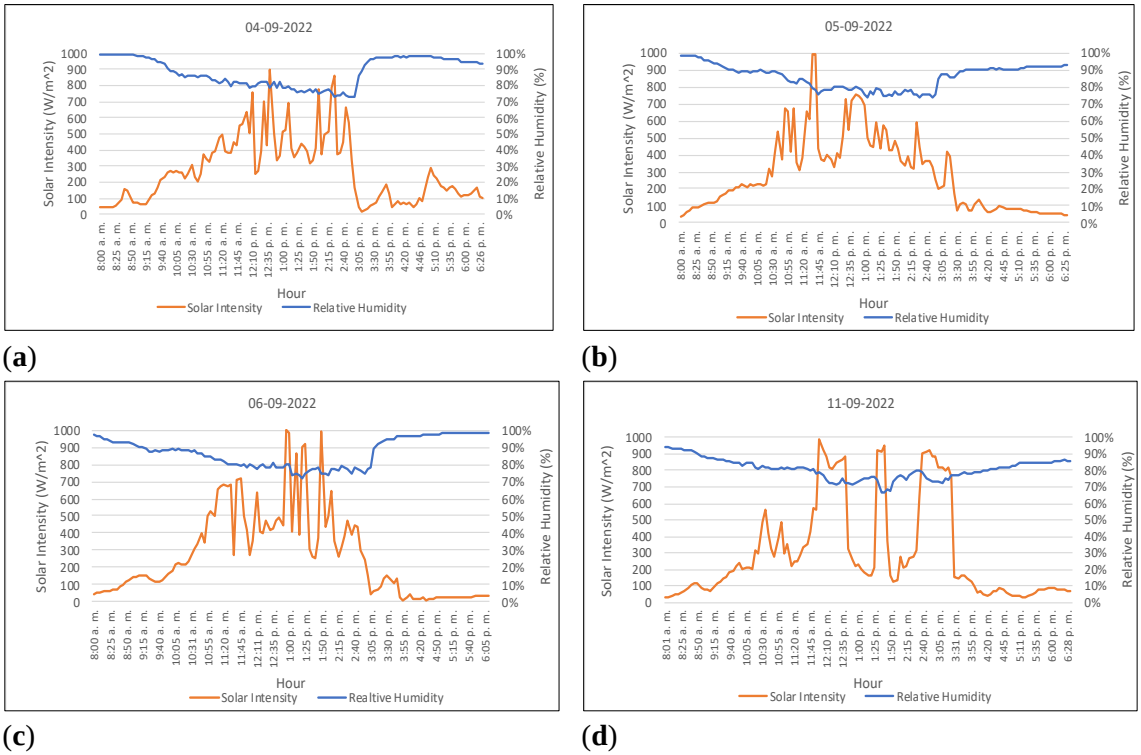

(**a**) (**b**)

(**c**) (**d**)

Figure 6. Behavior of solar intensity and relative humidity, group 2: (a) 09/04/2022, (b) 09/05/2022, (c) 09/06/2022, and (d) 09/11/2022.

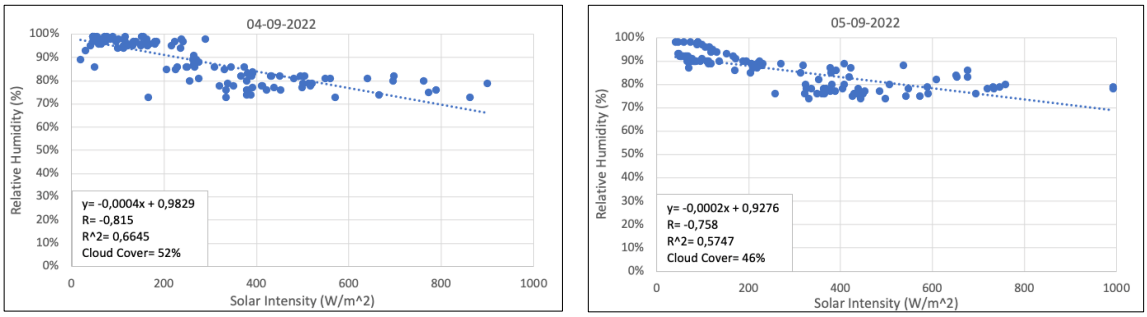

(**a**) (**b**)

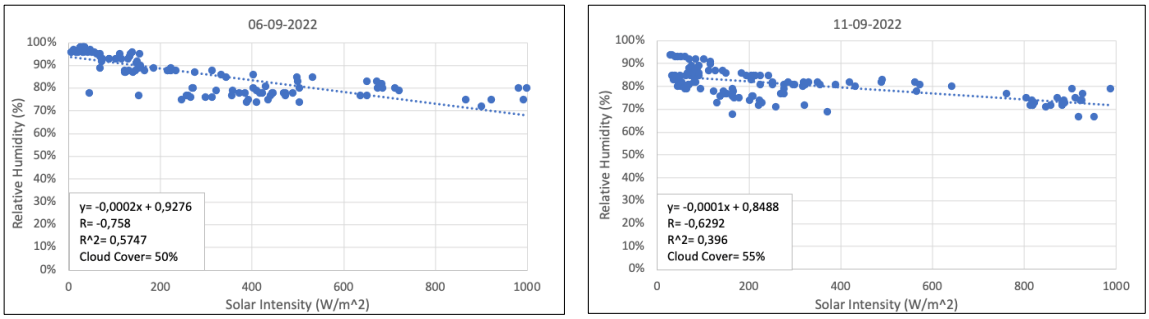

(**c**) (**d**)

Figure 7. Linear regression model and cloud cover, group 2: (a) 09/04/2022, (b) 09/05/2022, (c) 09/06/2022, and (d) 09/11/ 2022.

For this data group, there were clearer mornings compared to those from group 1, mid-days with high cloud cover, and afternoons with rain events. On September 4, 5, and 6 between 8:00 and 11:00 am the cloud cover was low and with small shadow intervals; however, from 11:00 am to 2:00 pm cloudiness increased considerably, alternating high peaks of shadow and solar intensity almost simultaneously. Unlike these days, September 11 had a different behavior both in the morning and at noon, with high cloudiness and longer cloudiness. Nonetheless, during the 4 days of this group there were rain events starting at 3:00 pm.

R values varied between -0.63 and -0.81, indicating that there is a negative linear correlation between moderate ($0.4 < R < 0.69$) and high ($0.7 < R < 0.89$) [53]. Nonetheless, and despite the high cloud cover (between 46 and 55%), the linear correlation was better when compared to that found for group 1, which may be because the shadow periods were less prolonged for group 2. In general, R^2 showed poor performance for the applied linear regression model.

Figures 8 and 9 show the behavior of solar intensity and relative humidity; and the linear regression model for the days of group 3, respectively.

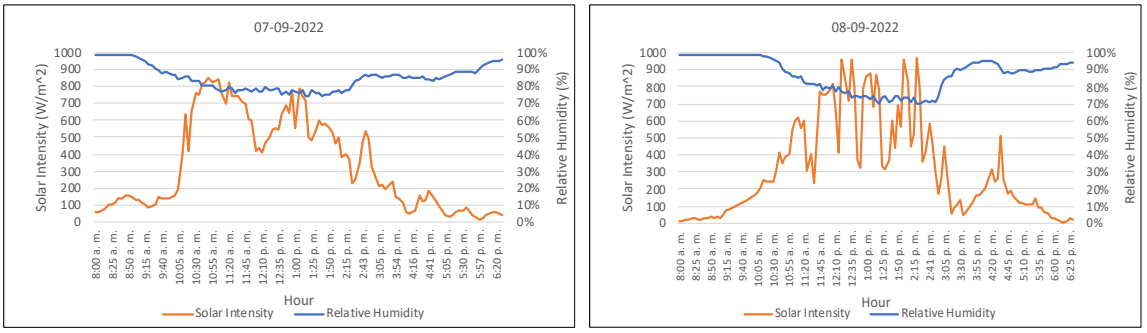

(**a**) (**b**)

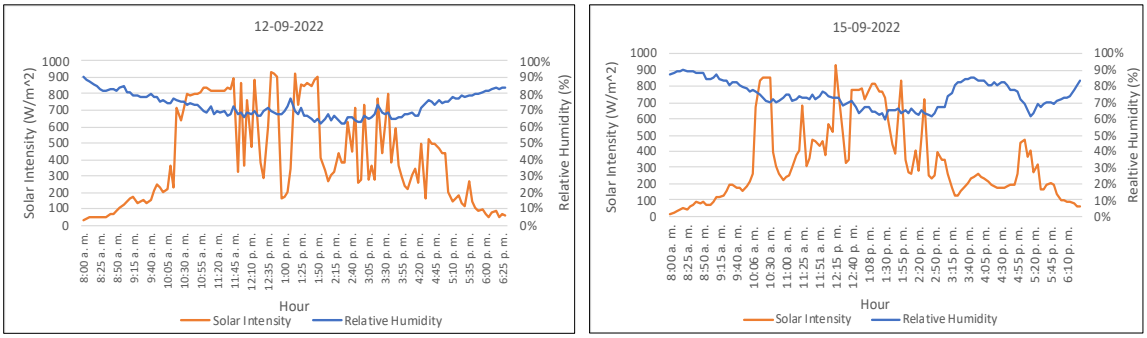

(**c**) (**d**)

Figure 8. Behavior of solar intensity and relative humidity, group 3: (a) 09/07/2022, (b) 09/08/2022, (c) 09/12/2022, and (d) 15/ 09/2022.

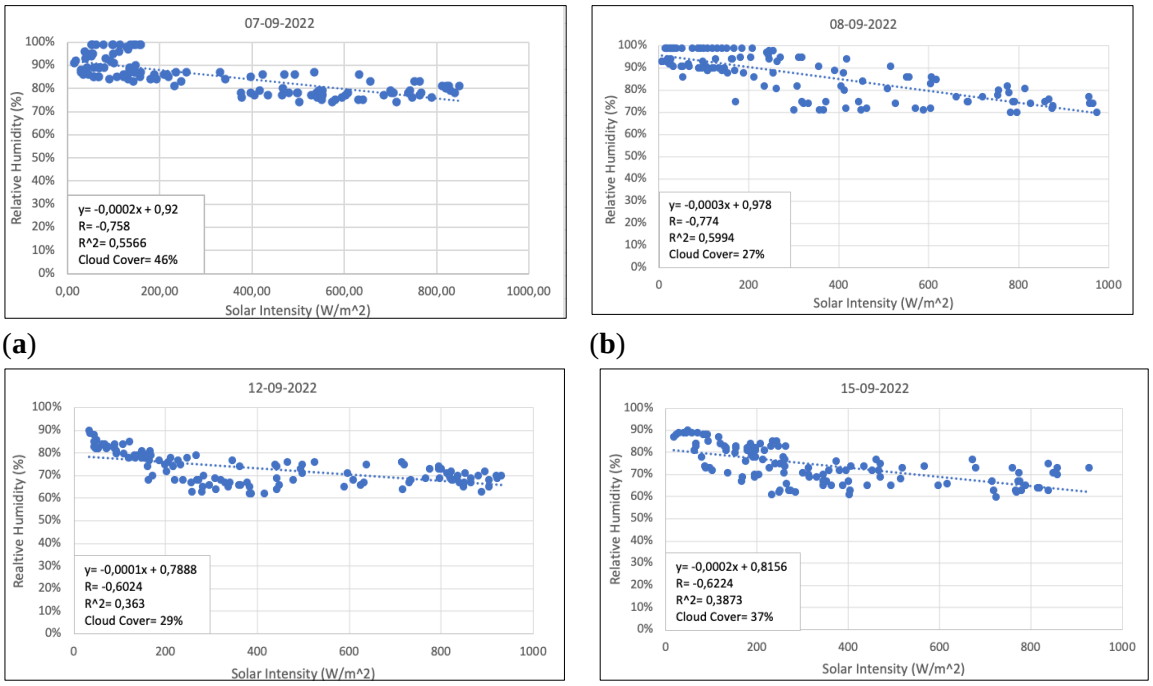

Figure 9. Linear regression model and cloud cover, group 3: (a) 09/07/2022, (b) 09/08/2022, (c) 09/12/2022 and (d) 09/15/2022.

This data group showed a very similar behavior to group 2, with clear mornings and low cloud cover; mid-days and afternoons with high cloud cover, but no rain events throughout the day. In the 4 days of this group, high solar intensity occurred between 10:30 am and 2:30 pm, with cloud coverage between 27% and 46%. The value of the R coefficient was between -0.60 and -0.76%, i.e., there is a negative linear correlation between moderate and high. However, R^2 showed poor performance for the applied linear regression model.

Finally, Figures 10 and 11 show, for group 4, the behavior of solar intensity and relative humidity, and the linear regression model, respectively.

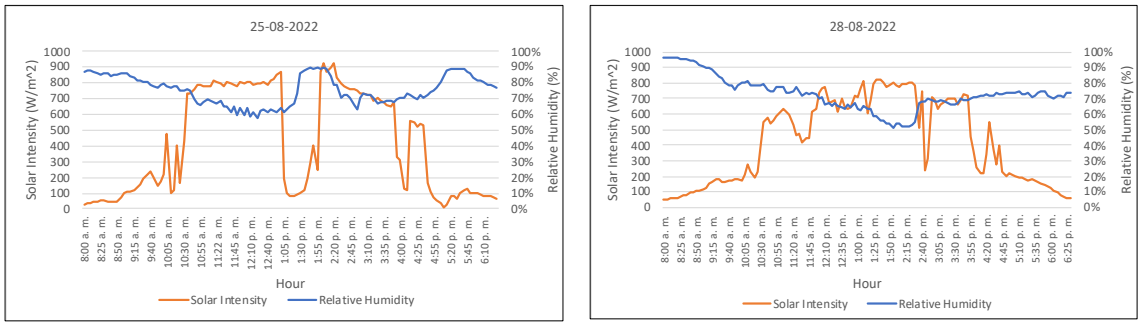

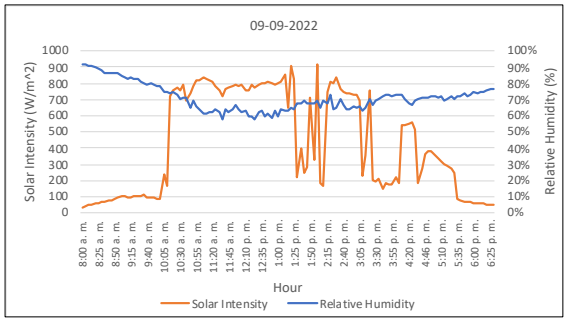

(**c**)

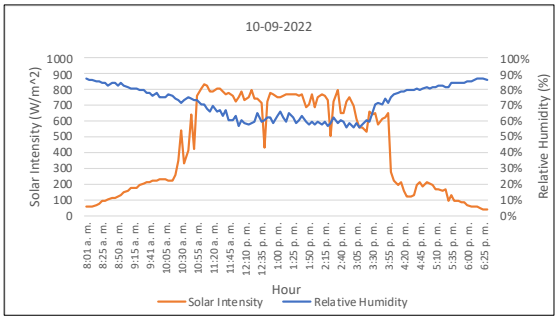

(**d**)

Figure 10. Behavior of solar intensity and relative humidity, group 4: (a) 08/25/2022, (b) 08/28/2022, (c) 09/09/2022, and (d) 10/ 09/2022.

The days of this group were characterized by having low cloud cover, by a total absence of rain events and by clear and sunny mornings. The highest and most prolonged solar intensities occurred in this group of days, mainly between 10:00 am and 3:30 pm, with values between 700 and 900 W/m^2. Although shadow peaks occurred, they were very punctual and for short periods, which did not significantly affect the warm environmental temperature of those days. The relative humidity was very similar between these days, presenting minimum values of 50 and 60% at midday.

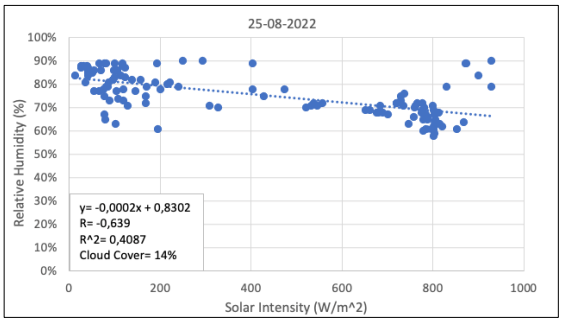

(**a**)

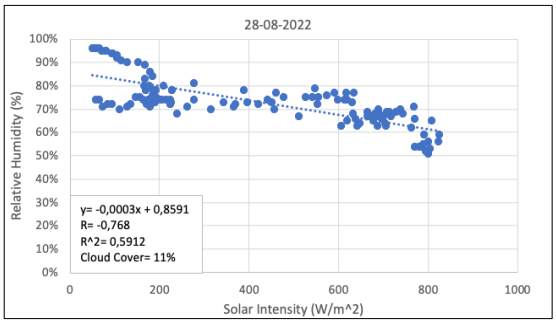

(**b**)

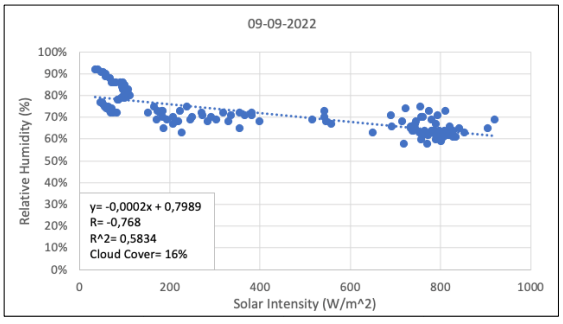

(**c**)

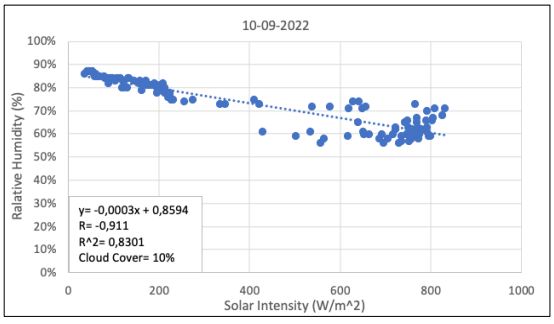

(**d**)

Figure 11. Linear regression model and cloud cover, group 3: (a) 08/25/2022, (b) 08/28/2022, (c) 09/09/2022 and (d) 09/10/2022.

The Pearson correlation coefficient, for August 25 and 28 and September 9, had a value between -0.64 and -0.77, indicating a moderate to high negative linear correlation. However, the R for September 10 was -0.91, i.e., on that day there was a very high negative linear correlation and the R^2 showed a very strong and excellent fit of the applied linear regression model [53]. This result could be due to the low cloud cover throughout that day (Cloud cover

= 10%), as well as the short duration of the shadow peaks that occurred. These results show that there is a very high negative correlation between solar intensity and relative humidity, if cloud cover and shadow periods are low and short, respectively. As cloud cover rises, the correlation R between relative humidity and solar intensity decreases, but remains inversely proportional, i.e., as solar intensity rises, relative humidity decreases.

3.2. Performance of the solar still as a function of Solar Intensity and Relative Humidity

The days in which the tests with the solar still were carried out were characterized by having sunny mornings but highly cloudy afternoons and even sporadic short-term rain events. Nonetheless, if we bear in mind the average values of solar intensity and relative humidity, the best solar still performance rates were obtained on days with high relative humidity (August 22 and 30, 2022), results consistent with what was stated by Kofi et al. [38]. On the other hand, with the performance rate of August 19 and 31, it was possible to corroborate that there is an inversely proportional correlation between solar intensity and relative humidity, which allows balancing the solar still performance, i.e., to the extent that the average solar intensity is high, the average relative humidity will be low (and vice versa), without this significantly altering the average performance of the solar still. However, rain events or high cloud cover with prolonged periods of time considerably affect solar radiation, and consequently, the general performance of solar still [10,20].

Table 3 lists the performance of the solar still used for the tests, based on the maximum and average solar intensity, during the days monitored.

Table 3. Solar still performance as a function of solar radiation.

Test Date	Maximum solar intensity (W/m^2)	Average solar intensity (W/m^2)	Minimum Relative Humidity (%)	Average Relative Humidity (%)	Production rate solar still (L/m^2-día)
19/08/2022	932.2	687.2	40.0	47.5	0.89
22/08/2022*	1016.6	577.8	58.0	73.3	1.30
30/08/2022	927.0	451.3	64.0	76.7	0.97
31/08/2022	876.7	367.5	60.0	74.7	0.88

*Rain event occurred in the afternoon, but with a sunny morning.

5. Conclusions

Based on the results obtained in this research, it is possible to affirm that there is a negative linear correlation between solar intensity and relative humidity, i.e., as solar intensity rises, relative humidity decreases. This correlation is strongly influenced by cloud cover and by the duration of the shadow over the site where the tests with the solar still are carried out. Thus, when the cloud cover is less than 10% and the shadow it produces over the test site is for short periods (between 5 and 10 minutes), it is possible to find correlation coefficients higher than -0.9, indicating that there is a very high negative linear correlation between these two climatic parameters. In this sense, the greater the average solar radiation, the greater the performance and production of fresh water in a solar still.

With this research, it is possible to affirm that one of the most important climatic factors in a solar still performance is undoubtedly solar radiation; however, a low and little prolonged cloud cover is necessary at the test site. On the other hand, it is also important to consider the average relative humidity of the site since this

climatic factor makes it possible to balance the overall performance of the distillation.

Funding: This Project has been supported by CONACyT (Mexican governmental agency), through the Scholarship with Registration Number 804395 (2021-2024).

References

1. Singh, D.B.; Singh, A.K.; Navneet, K.; Dwivedi, V.K.; Yadav, J.K.; Singh, G. Performance analysis of special design single basin passive solar distillation systems: A comprehensive review. In Advances in Engineering Design. Lecture Notes in Mechanical Engineering, 1st ed.; Prasad, A., Gupta, S., Tyagi, R., Eds.; Springer: Singapore, 2019; 301–310. https://doi.org/10.1007/978-981-13-6469-3_27.
2. Singh, S.K.; Kaushik, S.C.; Tyagi, V.V.; Tyagi, S.K. Comparative Performance and parametric study of solar still: A review. Sustain. Energy Technol. Assess **2021**, 47, 1015541. https://doi.org/10.1016/j.seta.2021.101541.
3. Nandi, A.; Megiddo, I.; Ashok, A.; Verma, A.; Laxminarayan, R. Reduced burden of childhood diarrheal diseases through increased access to water and sanitation in India: A modeling analysis. Soc. Sci. Med. **2017**, 180, 181–192. https://doi.org/10.1016/j.socscimed.2016.08.049.
4. Gugulothu, R.; Somanchi, N.S.; Devi, R.S.R.; Banoth, H.B. Experimental Investigations on Performance Evaluation of a Single Basin Solar Still Using Different Energy Absorbing Materials. Aquat. Procedia **2015**, 4, 1483–1491. https://doi.org/10.1016/j.aqpro.2015.02.192.
5. Isah, A.S.; Shafiai, S.H.; Takaijudin, H.B.; Singh, B.S.; Haq-Gilani, S.I. The role of desalination and contribution of hybrid solar desalination system towards primary health care. Case Stud. Therm. Eng. **2022**, 6, 100253. https://doi.org/10.1016/j.cscee.2022.100253.
6. Esmaeilion, F.; Ahmadi, A.; Hoseinzadeh, S.; Aliehyaei, M.; Makkeh, S.A.; Astiaso Garcia, D. Renewable energy desalination; a sustainable approach for water scarcity in arid lands. Inter. J. Sustain. Eng. **2021**, 14, 6, 1916-1942. https://doi.org/10.1080/19397038.2021.1948143.
7. Sharshir, S.W.; Yang, N.; Peng, G.; Kabeel, A.E. Factors affecting solar stills productivity and improvement techniques: A detailed review. Appl. Therm. Eng. **2016**, 100, 267-284, https://doi.org/10.1016/j.applthermaleng.2015.11.041.
8. Aybar, H.S.; Assefi, H. A review and comparison of solar distillation: Direct and indirect type systems. Desalination Water Treat. **2009**, 10, 1–3, 321–331. https://doi.org/10.5004/dwt.2009.931.
9. Muftah, A.F.; Alghoul, M.A.; Fudholi, A.; Abdul-Majeed, M.M.; Sopian, K. Factors affecting basin type solar still productivity: A detailed review. Renew. Sustain. Energy Rev. **2014**, 32, 430-447, https://doi.org/10.1016/j.rser.2013.12.052.
10. Abujazar, M.S.S.; Fatihah, S.; Rakmi, A.R.; Shahrom, M.Z. The effects of design parameters on productivity performance of a solar still for seawater desalination: A review. Desalination **2016**, 385, 178-193. https://doi.org/10.1016/j.desal.2016.02.025.
11. Pangwa, N.; Msomi, V. Progress made in eliminating factors affecting solar stills productivity, Mater Today: Proc. **2022**, 57, 2, 969-974. https://doi.org/10.1016/j.matpr.2022.03.300.
12. Prakash, P.; Velmurugan, V. Parameters influencing the productivity of solar stills.

A review. Renew. Sustain. Energy Rev. **2015**, 49, 585-609. https://doi.org/10.1016/j.rser.2015.04.136.

13. Feria-Díaz, J.J.; López-Méndez, M.C.; Ortiz-Monterde, L.; Médina-Salgado, B.A.; Perez-Rosas, N.C. Performance Evaluation of Solar Still in Veracruz, Mexico Gulf Coastline. Water **2022**, 14, 1567. https://doi.org/10.3390/w14101567.
14. Jathar, L.D.; Ganesan, S.; Shahapurkar, K.; Soudagar, M.E.M.; Mujtaba, M.A.; Anqi, A.E.; Farooq, M.; Khidmatgar, A.; Goodarzi, M.; Safaei, M.R. Effect of various factors and diverse approaches to enhance the performance of solar stills: a comprehensive review. J. Therm. Anal. Calorim. **2022**, 147, 4491-4522. https://doi.org/10.1007/s10973-021-10826-y.
15. Muthu-Manokar, A.; Kalidasa-Murugave, K.; Esakkimuthu, G. Different parameters affecting the rate of evaporation and condensation on passive solar still - A review. Renew. Sustain. Energy Rev. **2014**, 38, 309-322. https://doi.org/10.1016/j.rser.2014.05.092.
16. Almuhanna, E.A. Evaluation of Single Slop Solar Still Integrated with Evaporative Cooling System for Brackish Water Desalination. J. Agric. Sci. **2014**, 6, 48-58. https://doi.org/10.5539/jas.v6n1p48.
17. Aburideh, H.; Deliou, A.; Abbad, B.; Alaoui, F.; Tassalit, D.; Tigrine, Z. An experimental study of a solar still: Application on the sea water desalination of Fouka. Proced. Engin. **2012**, 33, 475–484. https://doi.org/10.1016/j.proeng.2012.01.1227.
18. Nafey, A.S.; Abdelkader, M.; Abdelmotalip, A.; Mabrouk, A. Parameters affecting solar still productivity. Energy Convers. Manag. **2000**, 41, 1797–1809. https://doi.org/10.1016/S0196-8904(99)00188-0.
19. Abdelkader, M.; Nafy, A.S.; Abdelmotalip, A.; Mabrouk, A. Experimental evaluation of solar still mathematical models. In Proceedings of the Fourth International Water Technology Conference, Alexandria, Egypt, 1999; 23–25.
20. Essa, F.A.; Abdullah, A.; Majdi, H.S.; Basem, A.; Dhahad, H.A.; Omara, Z.M.; Mohammed, S.A.; Alawee, W.H.; Ezzi, A.A.; Yusaf, T. Parameters Affecting the Efficiency of Solar Stills—Recent Review. Sustainability **2022**, 14, 10668. https://doi.org/10.3390/su141710668.
21. Okeke, C.; Egarievwe, S.; Animalu, A. Effects of coal and charcoal on solar-still performance. Energy **1990**, 15, 11, 1071–1073. https://doi.org/10.1016/0360-5442(90)90035-Z.
22. Ghoneyem, A.; Lleri, A. Software to analyze solar stills and an experimental study on the effects of the cover. Desalination **1997**, 114, 37–44. https://doi.org/10.1016/S0011-9164(97)00152-5.
23. El-Sebaii, A.A. Effect of wind speed on active and passive solar stills. Energy Convers. Manag. **2004**, 45, 7–8, 1187–1204. https://doi.org/10.1016/j.enconman.2003.09.036
24. Murugavel, K.K.; Sivakumar, S.; Ahamed, J.R.; Chockalingam, K.K.S.K.; Srithar, K. Single basin double slope solar still with minimum basin depth and energy storing materials. Appl. Energy **2010**, 87, 2, 514–523. https://doi.org/10.1016/j.apenergy.2009.07.023.
25. Bhargva, M.; Yadav, A. Factors affecting the performance of a solar still and productivity enhancement methods: A review. Environ. Sci. Pollut. Res. **2021**, 28, 54383-54402.

https://doi.org/10.1007/s11356-021-15983-z.
26. Xiao, G.; Wang, X.; Ni, M.; Wang, F.; Zhu, W.; Luo, Z.; Cen, K. A review on solar stills for brine desalination. Appl. Energy **2013**, 103, 642–652. http://dx.doi.org/10.1016/j.apenergy.2012.10.029.
27. Rashidi, S.; Esfahani, J.A; Rahbar, N. Partitioning of solar still for performance recovery: experimental and numerical investigations with cost analysis. Sol. Energy, **2017**, 153, 41–50. https://doi.org/10.1016/j.solener.2017.05.041.
28. Malik, M.A.S.; Tiware, G.N.; Kumar, A.; Sodha, M.S. Solar distillation, 1st ed; Pergamon Press: Oxford, United Kingdom, 1982; 255-312
29. Al-Hinai, H.; Al-Nassri, M.S.; Jubran, B.A. Effect of climatic, design and operational parameters on the yield of a simple solar still. Energy Convers. Manag. **2002**, 43, 13, 1639–1650. https://doi.org/10.1016/S0196-8904(01)00120-0
30. Reddy, R.M.; Reddy, K.H. Upward heat flow analysis in basin type solar still. J. Min. Metall. **2009**, 45, 121-126.
31. Castillo-Téllez, M.; Pilatowsky-Figueroa, I.; Sánchez-Juárez, A.; Fernández-Zayas, J.L. Experimental study on the air velocity effect on the efficiency and freshwater production in a forced convective double slope solar still. Appl. Therm. Eng. **2015**, 75,1192–200. https://doi.org/10.1016/j.applthermaleng.2014.10.032.
32. Shahid, A.; Huang, H.L.; Khalique, C.M.; Bhatti, M.M. Numerical analysis of activation energy on MHD nanofluid flow with exponential temperature-dependent viscosity past a porous plate. J. Therm. Anal. Calorim. **2020**, 143, 2585–2596. https://doi.org/10.1007/ s10973-020-10295-9.
33. Bhatti, M.M.; Abdelsalam, S.I. Thermodynamic entropy of a magnetized Ree-Eyring particle-fluid motion with irreversibility process: A mathematical paradigm. Appl. Math. Mech. **2020**, 33, 1–17. https://doi.org/10.1002/zamm.202000186.
34. Zamfir, E.; Oancea, C.; Badescu, V. Cloud cover influence on long-term performances of flat plate solar collectors. Renew. Energy **1994**, 4, 3, 339–347. https://doi.org/10.1016/0960-1481(94)90038-8.
35. El-Nashar, A.M. Seasonal effect of dust deposition on a field of evacuated tube collectors on the performance of a solar desalination plant. Desalination **2009**, 239, 1–3, 66–81. https://doi.org/10.1016/j.desal.2008.03.007.
36. Lindblom, J.; Nordell, B. Water production by underground condensation of humid air. Desalination **2006**, 189, 248–260. https://doi.org/10.1016/j.desal.2005.08.002.
37. Kalidasa-Murugavel, K.; Anburaj, P.; Samuel-Hanson, R.; Elango, T. Progresses in inclined type solar stills. Renew. Sust. Energ. Rev. **2013**, 20, 364-377. https://doi.org/10.1016/j.rser.2012.10.047.
38. Koffi, B.K.; Konan, D.K.; Nguessa, R.K.; Saraka, J.K.; Tanoh, A.; Kouacou, M.A.; Yeo, Z.; Koua, A.A. Modeling of solar still for Production of Pure Water in the Abidjan Zones. Modelling of Solar Still for Production of Pure Water in the Abidjan Zones. Res. J. Phys. **2009**, 3, 5–13. https://doi.org/10.3923/rjp.2009.5.13.
39. Rodríguez-Macedo, M.; González-Christen, A.; León-Paniagua, L.S. Diversity of wild mammals of Misantla, Veracruz, México. Rev. Mex. Biodivers. **2014**, 85, 1, 262–275. https://doi.org/10.7550/rmb.36143.
40. Kim, H.C., & Hofmann, E.E. Evaluation and derivation of cloud-cover algorithms

for calculation of surface irradiance in sub-Antarctic and Antarctic environments. Antarct. Sci. **2005**, 17,1, 135–149. https://doi.org/10.1017/S0954102005002518.

41. Jamil, M.A.; Yaqoob, H.; Farooq, M.U.; Teoh, Y.H.; Xu, B.B.; Mahkamov, K.; Sultan, M.; Ng, K.C.; Shahzad, M.W. Experimental Investigations of a Solar Water Treatment System for Remote Desert Areas of Pakistan. Water **2021**, 13, 1070.
42. Laevastu, T., Factors effecting the temperature of the surface layer of the sea. Comment. Phys. Math. **1960**, 25, 1, 1-136.
43. Kasten, F.; Czeplak, G. Solar and terrestrial radiation dependent on the amount and type of cloud. Sol. Energy **1980**, 24,2, 177–189. https://doi.org/10.1016/0038-092X(80)90391-6.
44. Dobson, F. W.; Smith, S.D. Bulk models of solar radiation at sea. Q.J.R. Meteorol. Soc. **1988**, 114, 479, 165–182. https://doi.org/10.1002/qj.49711447909.
45. Davis, R.F. Comparison of modeled to observed global irradiance. J. Appl. Meteorol. **1996**, 35, 192-201. https://doi.org/10.1175/1520-0450(1996)035<0192:COMTOG>2.0.CO;2.
46. Sutter, M., Dürr, B.; Philipona, R. Comparison of two radiation algorithms for surface-based cloud-free sky detection. J. Geophys. Res. Atmos. **2004**, 109,17. https://doi.org/10.1029/2004JD004582.
47. Elango, C.; Gunasekaran, N.; Sampathkumar, K. Thermal models of solar still—A comprehensive review. Renewable Sustainable Energy Rev. **2015**, 47, 856–911.
48. Khan, S.; Ali Khan, M.; Zafar, A.; Javed, M.F.; Aslam, F.; Musarat, M.A.; Vatin, N.I. Predicting the Ultimate Axial Capacity of Uniaxially Loaded CFST Columns Using Multiphysics Artificial Intelligence. Materials **2022**, 15, 39.
49. Alade, I.O.; Bagudu, A.; Oyehan, T.A.; Abd Rahman, M.A.; Saleh, T.A.; Olatunji, S.O. Estimating the refractive index of oxygenated and deoxygenated hemoglobin using genetic algorithm–support vector regression model. Comput. Methods Programs Biomed. **2018**, 163, 135–142.
50. Aldrees, A.; Khan, M.A.; Tariq, M.A.U.R.; Mustafa Mohamed, A.; Ng, A.W.M.; Bakheit Taha, A.T. Multi-Expression Programming (MEP): Water Quality Assessment Using Water Quality Indices. Water **2022**, 14, 947.
51. Nafees, A.; Amin, M.N.; Khan, K.; Nazir, K.; Ali, M.; Javed, M.F.; Aslam, F.; Musarat, M.A.; Vatin, N.I. Modeling of Mechanical Properties of Silica Fume-Based Green Concrete Using Machine Learning Techniques. Polymers **2022**, 14, 30.
52. Mongomery, D.C. Design and Analysis of Experiments, 10th Ed.; John Willy & Sons: Hoboken, New Yersey, USA, 2019, ISBN: 978-1-119-49244-3.
53. Lind, D.A.; Marchal, W.G.; Wathen, S.A. Statistical Techniques in Business & Economics, 15th ed.; McGrawHill: México D.F., México, 2012; pp. 465-472.